Sigma Journal of Engineering and Natural Sciences
Web page info: https://sigma.yildiz.edu.tr
DOI: 10.14744/sigma.2025.1915

Research Article

Analysis on the mechanical aspects of a multi-layered structure constructed from 1.14 Cr-1.0 Mo steel utilizing flux-cored wire by means of GMAW-based WAAM

Vaishali PRAJAPATI[1,*], Vyomesh BUCH[1]

[1]Department of Mechanical Engineering, Parul Institute of Technology, Parul University, Vadodara, Gujarat, 391760, India

ARTICLE INFO

Article history
Received: 29 March 2025
Revised: 01 June 2025
Accepted: 11 September 2025

Keywords:
Gas Metal Arc Welding (GMAW), 1.14 Cr-1.0 Mo Steel; Multi-Layered Formations; Wire-Arc Additive Manufacturing (WAAM Mechanical Aspects)

ABSTRACT

In the present work, flux-cored wires of 1.14 Cr-0.5 Mo steel were used to manufacture a multi-layered structure under optimal process parameters using a wire-arc additive manufacturing (WAAM) technique based on gas metal arc welding (GMAW). Optimal parameters were obtained through the passing vehicle search (PVS) algorithm. The multi-layered structure was studied to evaluate its small- and large-scale features, as well as its strength and toughness at different locations within the structure. Microstructures of ferrite and pearlite, typical of low-alloy steels, were observed. A higher proportion of columnar grains and larger uniform grains were noted in the middle portion compared with the bottom. Macrostructural analysis in many regions confirmed defect-free geometries. The two layers were well connected, producing perfect oxidation-free fusion. Furthermore, chrome molybdenum steel exhibited an ultimate tensile strength (UTS) of 890 MPa and a yield strength (YS) of 712 MPa, while GMAW-produced chrome molybdenum steel achieved a UTS of 910 MPa and a YS of 728 MPa. All tensile properties determined by WAAM for the upper and lower zones were within the specified range. Compared with commercially available chrome moly steel, the average impact energy of 5.3 J demonstrated satisfactory strength. These results indicate that the structure fabricated using the GMAW-based WAAM technique meets industrial application requirements.

Cite this article as: Prajapati V, Buch V. Analysis on the mechanical aspects of a multi-layered structure constructed from 1.14 Cr-1.0 Mo steel utilizing flux-cored wire by means of GMAW-based WAAM. Sigma J Eng Nat Sci 2026;44(3):2082−2090.

INTRODUCTION

Traditional manufacturing, characterised by costly and less efficient processes that generate considerable material waste, is becoming increasingly outdated for fabricating metal parts. Additive manufacturing (AM) has emerged as a solution to overcome these challenges. Initially developed for plastic materials, AM could not produce mechanically robust parts. Consequently, metal AM has been introduced [1]. Metal AM deposits material

***Corresponding author.**
*E-mail address: 212300471002@paruluniversity.ac.in

This paper was recommended for publication in revised form by Editor-in-Chief Ahmet Selim Dalkilic

Published by Yıldız Technical University Press, İstanbul, Turkey

layer by layer to create components with high strength while reducing costs by approximately 50%. It is increasingly demanded in aerospace, automotive, defence, biomedical, and electronics industries [2]. Metal 3D printing primarily relies on laser or powder bed fusion techniques. Among AM approaches, gas metal arc welding (GMAW) has gained significant attention. Wire arc additive manufacturing (WAAM), a direct energy deposition method in AM, offers high deposition rates, favourable mechanical properties, and relatively low equipment costs. WAAM can be implemented using various energy sources such as gas tungsten arc welding and plasma arc welding [3]. While many AM techniques are expensive, WAAM is cost-effective and well suited for mass production. It is a wire-feed process integrated with automated computer systems [4][5]. Deposition rates as high as 8 kg/h have been reported for GMAW-based WAAM, ensuring improved dimensional precision [6]. To achieve high surface quality, post-machining is often required, in addition to optimizing parameters such as voltage, travel speed, and gas mixture ratio [7][8]. Ji et al. highlighted that AM is a valuable method to produce complex parts with minimal tooling, and modern 3D printing technologies further enhance these capabilities. The growing demand for advanced manufacturing highlights the need to create complex formations that minimise waste, time, and costs, while achieving higher deposition rates, improved energy efficiency, enhanced strength, and better geometric accuracy. These advantages make AM systems highly attractive for industrial applications.

1.14 Cr-1.0 Mo stainless steel exhibits excellent mechanical properties and corrosion resistance due to its Mo, Ni, and Cr content [9]. SS 316L, another low-carbon austenitic stainless steel with 0.03% carbon, also demonstrates superior weldability and fusion at temperatures between 1300°C and 1400°C [10]. Owing to its high deposition rate in GMAW, SS 316L offers corrosion resistance, high strength, and good weldability, making it suitable for nuclear, biological, marine, petrochemical, and shipbuilding applications [11].

Jin et al. [12] studied the WAAM process on stainless steel alloys and found that process parameters significantly influenced strength, microstructure, and layer formation. Experimental results showed the necessity of optimizing physical metallurgy mechanisms, post-heat treatment, and process parameters. Chen et al. [13] investigated the GMAW-based additive manufacturing of SS 316L and concluded that heat treatment affected tensile strength and corrosion resistance. A 1000°C thermal treatment enhanced both yield and tensile strength. Queguineur et al. [14] analysed metallurgical and mechanical properties using two different materials, demonstrating improvements in tensile strength and corrosion resistance. Ahsan et al. [15] applied the GMAW process to fabricate bi-metallic structures using SS 316L and low-alloy carbon steel, reporting defect-free welded zones. The stainless-steel zone exhibited higher microhardness due to its Cr content. Lee et al. [16] examined heat accumulation in SS 316L during WAAM through experimental and numerical methods, finding excellent yield strength and hardness under cold metal transfer conditions. Wahsh et al. [17] reported successful layer-by-layer deposition of aluminium using GMAW, with minimal heat input, no spatter, cracks, or significant porosity. However, after extensive testing, the process settings were adjusted to enhance the shape of the weld bead, leading to better small and large structures, heat distribution, and other mechanical properties. Le and Mai [18] demonstrated that WAAM-fabricated 308L components presented adequate mechanical strength and hardness, despite some anisotropy in mechanical properties. Fang [19] studied high-strength low-alloy steel produced via GMAW-based WAAM at a deposition rate of 4.5 kg/h. Impact testing and microstructure characterization were conducted at low temperatures. The part's microstructure consists of both granular and lower bainite. At room temperature, the AM-generated component has a sufficient strength-ductility balance. Upon testing, the ultimate tensile strength, yield strength, and elongation at fracture were found to be within the ranges of 830–850 MPa, 765–770 MPa, and 18.3–22.8%, respectively.

Long and Wen reported the effects of WAAM process parameters on material properties. The process parameters primarily influence the material's microstructure and overall performance by altering the energy input and cooling rate of the molten pool. To better understand the mechanism of the WAAM process, it has been noted in low-alloy steel, an increased cooling rate and a decreased energy input are directly proportional to increment in UTS and YS [20].

Shalini et al. investigated the effect of interlayer delays of 20, 40, and 80 s during WAAM wall fabrication, reporting improved density, reduced wall width and height, and refined grain structures with increasing interlayer delay [21].

Optimization methods such as differential evolution, particle swarm optimization, and cuckoo search are commonly used for complex manufacturing challenges. However, genetic algorithms have limitations such as weak local search capability and slower convergence [22].

To address this, optimization in the present study was performed using the PVS algorithm, a metaheuristic approach similar to Teaching-Learning-Based Optimization (TLBO), but without requiring algorithm parameters.

The ductility of 316L stainless steel diminished due to a steady rise in ferrite concentration. These ferrites will impede the unrestricted movement of dislocations [23].

As layers are deposited, effective heat transmission declines as the temperature of the prior layer lowers the gradient of thermal energy. Whereas heat also escapes by convection and radiation, these methods are less efficient than conduction, which causes increased heat storage and a reduced cooling rate. Numerical models revealed that as building height increases, the temperature gradient diminishes and heat diffusion conditions deteriorate. A low cooling rate indicates inadequate dissipation of heat energy from the deposited walls, resulting in the production of coarse columnar grains alongside certain dendritic grains. [24] Consequently, the mechanical properties (ultimate tensile strength, yield strength, elongation, fatigue strength, and microhardness) of the manufactured component deteriorate.

A superalloy with a nickel-Kumar s. researched with a chromium alloy ratio of 15CR85S is used for the reactor part of this experiment, and 20CR80S is used for the furnace part. The plasma arc welding method operates at a temperature of 10,000°C with a coating layer of 75 microns on the materials. Although solid wire is frequently used in gas arc flux welding, tubular core wire can enhance current density and deposition rate.

Flux-cored wires can also be strengthened by the shielding flux within the core. Compared with solid wires, they are more effective and capable of welding thicker materials at higher speeds. Flux-core wire is an excellent option for high-strength mechanical joints, corrosion resistance, high-temperature tolerance, and environmentally sensitive applications. It provides molten pool reinforcement, greater material composition flexibility, and reduced porosity. A comprehensive examination of the process and the resulting products is required. Consistent with this need, the flux-cored wire arc additive manufacturing technique and the component composed of 1.14 Cr-0.5 Mo with optimal parameters were analysed. The GMAW-based WAAM process, which uses flux-cored 1.14 Cr-0.5 Mo steel wire, has not yet fully demonstrated its multi-layer formation, indicating potential for further material research. This study examines the microstructure, macrostructure, tensile testing, and impact testing of chrome moly steel. The findings are deemed crucial for future research and industrial applications. The authors declare that the present research can address industrial challenges related to the production of multi-layer structures and the evaluation of their mechanical characteristics.

The aim of this study is to explore the potential of wire arc additive manufacturing using tubular wire E81T1-B6C (diameter: 1.14 mm) as the starting material and to analyse the resulting formations. This objective was achieved through tensile testing, impact testing, and detailed macrostructural and microstructural characterization.

MATERIALS AND METHODS

Experimental Setup and Plan

This research utilised a WAAM configuration with the GMAW method to build a multi-layered structure using a Miller make KEMMPPI PRRO MIG-530 system. The raw material used was 1.14 Cr-0.5 Mo, which is specifically employed for welding chromoly steels in multiple or multi-pass welding. Figure 1 illustrates the experimental apparatus used in this investigation. A multi-layered structure with a diameter of 1.14 mm was fabricated using flux-cored wire of 1.14 Cr-0.5 Mo. The primary functions of the flux are to protect molten metal from the atmosphere, slow down the solidification rate (facilitating the release of gases and non-metallic impurities), regulate chemical composition, and refine the metal.

Table 1 shows the chemical composition of the substrate and infill wire. The raw material was deposited on a substrate plate using a torch, and the plate was fixed to the worktable during the deposition procedure.

In our most recent study, we conducted a parametric analysis by performing single-layer deposition and applying a passing vehicle search (PVS) algorithm. The present investigation focuses on constructing a multi-layered structure using optimised parameters for microstructure, macrostructure, and mechanical properties. Table 2 presents the optimised parameters used to fabricate the multi-layered formation.

Testing Characterization

Microstructure, macrostructure, and mechanical properties of the multi-layered formation were assessed at different locations on the top and bottom regions of the structure. Wire electrical discharge machining (WEDM) was used to prepare specimens for mechanical and metallographic evaluation. Specimens were polished sequentially using abrasive papers of grit sizes 240, 400, 600, 800, 1000, 1200, and 2000, followed by final polishing with alumina paste on a cloth to achieve a mirror finish. The samples were etched in a solution of hydrochloric acid (HCl), nitric acid (HNO_3), and glycerol ($C_3H_8O_3$) in the ratio 40:20:40 for two minutes to reveal finer microstructural and macrostructural features. An optical microscope (RADICAL instrument) was used to analyse microstructure, while a macroscope (IMS-300-TNC) was used for macrostructural analysis. Comprehensive mechanical testing, including tensile and impact examinations, was performed at different locations of the structure. WEDM was again employed to prepare tensile and impact specimens. Tensile specimens

Table 1. Chemical composition of 1.14-mm E81T1-B6C/M 4-6 % Cr 0.45-0.65% molybdenum

Grade	C	Mn	Si	P	S	Cr	Ni	Mo
	0.06	0.29	0.36	0.007	0.011	4.45	0.05	0.48

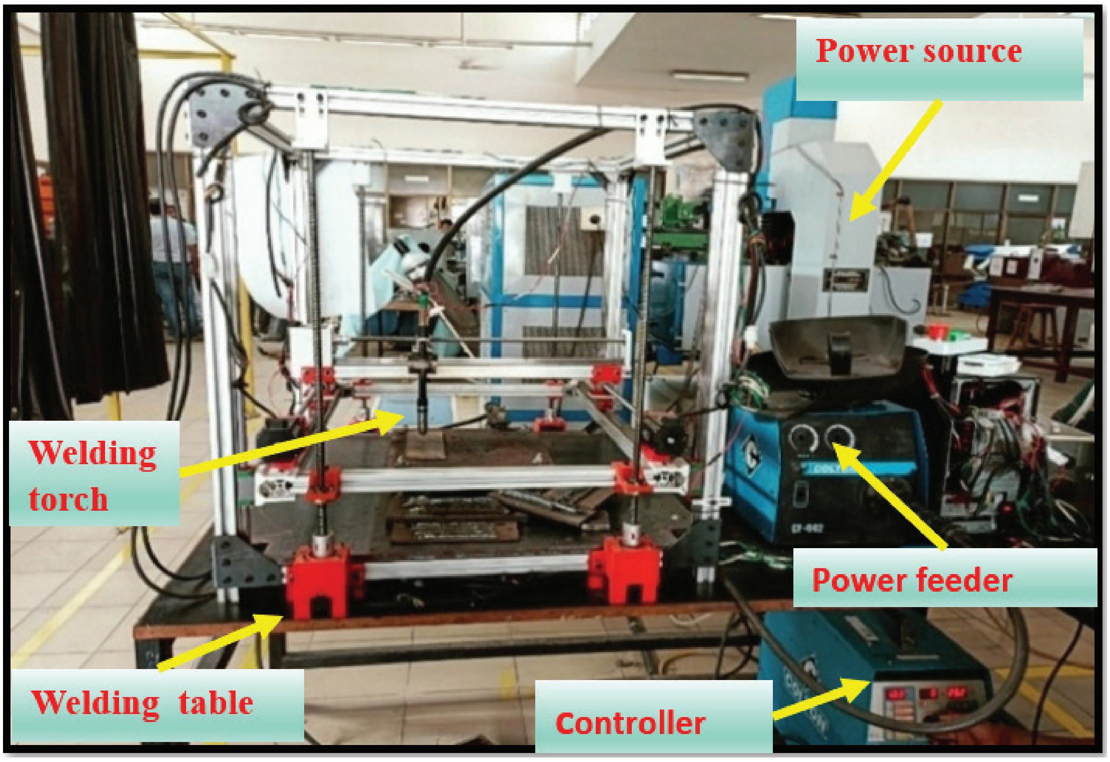

Figure 1. Experimental set up.

were prepared according to ASTM A370 standards and tested using an M-100 universal testing machine. Impact testing was carried out with an AIT-300 Charpy impact testing machine at room temperature. The Charpy specimens measured 55 mm × 10 mm × 3.3 mm. Figure 2 shows the schematic of impact testing locations.

RESULTS AND DISCUSSION

Construction of a Multi-Layered Structure

The optimization technique provided the parameters used to construct the structure. Identical bead-on-bead deposition produced a consistent multi-layered formation. To minimise residual stresses and deformation between layers, a cooling interval of 15 seconds was applied, which also facilitated solidification between successive layers.

Table 2. Optimised parameters for multi-layer formation

Sr. No.	Design variable	Value
1	Travel speed	30 mm/min
2	Voltage	23V
3	Gas mixture ratio	5
4	Gas flow rate	15 L/min
5	Arc length	90 mm

The fabricated structure was free from disbonding, and the layers exhibited seamless bonding between adjacent deposits. A small quantity of surface metal lumps was observed, but these could be easily removed during post-processing. Thus, WAAM with the GMAW method successfully produced a thin, multi-layered structure of the required quality on an E81T1-B6 substrate using the optimised parameters. Mechanical properties, macrostructure, and microstructure of the formation were subsequently analysed at different surface locations.

Macrostructural Characterization

A section was cut from the multi-layered formation for macrostructural analysis. Chemical etching (CHE) involves controlled chemical reactions between the surface and etchants to produce a smooth and observable surface. Common etchants include hydrochloric acid (HCl), sulfuric acid (H_2SO_4), nitric acid (HNO_3), hydrofluoric acid (HF), oxalic acid ($(COOH)_2$), and aqua regia (HCl + HNO_3). These acids are dissolved in water to the required concentrations [23]. The part was then polished sequentially with 240, 400, 600, 800, 1000, 1200, and 2000 grit abrasive papers, followed by 0.5-micron alumina paste on cloth to produce a smooth, mirror-like surface. Etching for 2 minutes in a mixture of glycerol ($C_3H_8O_3$), nitric acid (HNO_3), and hydrochloric acid (HCl) in the ratio of 40:20:40 revealed the macrostructure. The results showed a comparable macrostructure formation and surface morphology (Fig. 3).

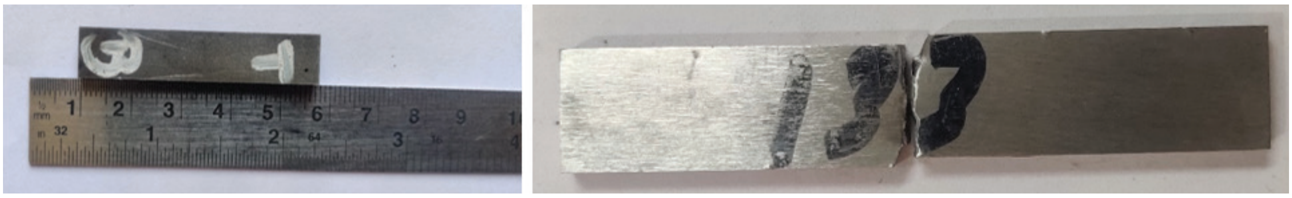

Figure 2. Impact specimen.

Figure 3. Sectional view of the multi-layered structure.

A strong bond between successive layers was observed, with no evidence of oxidation or defects. The macrostructure across different zones confirmed acceptable geometries. The WAAM process using flux-cored wire produced shallow, wide, circularly shaped layers. No internal defects were detected, aside from a thin slag layer on the surface [24].

Microstructural Characterization

The microstructure varied along the deposition direction due to thermal gradients arising during the process. Columnar grains developed in regions with strong heat flow, namely: (1) between the substrate and deposition wall, (2) between the surrounding air and deposition wall, (3) between the shielding gas and deposition wall, and (4) between successive layers. Variations in thermal history caused differences in grain size, with smaller grains in the bottom region and larger columnar grains toward the top. The absence of reheating in the final layers led to the formation of equiaxed grains at the surface [24]. The microstructure at the bottom region is primarily composed of evenly spaced grains that are relatively small. The middle region is also mainly made up of evenly distributed grains; however, the number of columnar grains and the size of the equiaxed grains are larger in this region than in the bottom region. In terms of the microstructure, the upper region differs significantly from the bottom region. In the upper section, equiaxed grains transform into columnar grains with strong directivity, and the grains become considerably larger (Fig. 4).

The distance between adjacent limbs of a dendrite, formed during the solidification of metals and alloys, is referred to as the dendrite arm spacing (DAS). It is influenced by solidification time, thermal gradients, and cooling rate, also affected microstructural uniformity. Smaller DAS values promoted consistent mechanical performance by enhancing durability and strength.

The microstructure was mainly composed of ferrite and pearlite, typical of low-alloy steels cooled slowly. Light regions corresponded to ferrite, while darker regions corresponded to pearlite. The pearlite was uniformly distributed with a fine morphology, contributing to balanced strength and ductility. The coexistence of ferrite and pearlite dendrites indicated varied cooling rates. The presence of ferrite in a columnar dendritic form indicates rapid cooling, during which ferrite solidifies in a directional manner. This formation can influence mechanical properties, potentially leading to anisotropy. The columnar dendritic formation in the coating suggests that the solidification process was controlled, whereas the pearlitic formation indicates that

Top Side

Bottom Side

Figure 4. Macrostructure at the top and bottom sides.

Bottom Zone Middle Zone Top Zone

Figure 5. Microstructure in the bottom, middle, and top zones (scale factor 10μm).

some areas cooled more slowly. Such variations in the microstructure can cause regional differences in mechanical properties, which may initiate fatigue cracks (Fig. 5).

Mechanical Characterization

Tensile examination

Tensile tests were conducted at multiple points of the multi-layered formation to evaluate mechanical properties. Specimens were prepared using WEDM as per ASTM E8M standards. All specimens exhibited elastic and plastic deformation prior to fracture. The average results for the top and bottom regions were: ultimate tensile strength (UTS) 910.68 MPa, yield strength (YS) 728.47 MPa, and elongation 3.92%. The variation in UTS and YS values showed an inverse relationship. Overall, the tensile properties of the WAAM-fabricated specimens were within the acceptable range for E81T1-B6 steel (Fig. 6).

Figure 6. Multi-layered formation prepared for characterizations.

Impact examination

The impact test was performed using an AIT-300 Charpy testing machine at room temperature. Charpy impact test specimens were prepared with dimensions of 55 mm × 10 mm × 5 mm. Figure 2 shows the schematic diagram of the testing locations and specimens used for impact testing. The specimens were prepared according to ASTM E340-15 standards for Charpy impact testing.

A 2 mm V-notch with a root radius of 0.25 mm was machined at a 45-degree angle in the centre of the sample for impact assessment. The test was conducted at room temperature. Samples from both the upper and lower zones were subjected to impact testing. The observed results indicated values of 4.7 J and 5.9 J for the upper and lower zone samples, respectively. The average result of 5.3 J indicates acceptable strength in comparison to commercially available chrome moly steel.If evaluated at full size, it will fall inside the acceptable range [25]. A slight variation in the

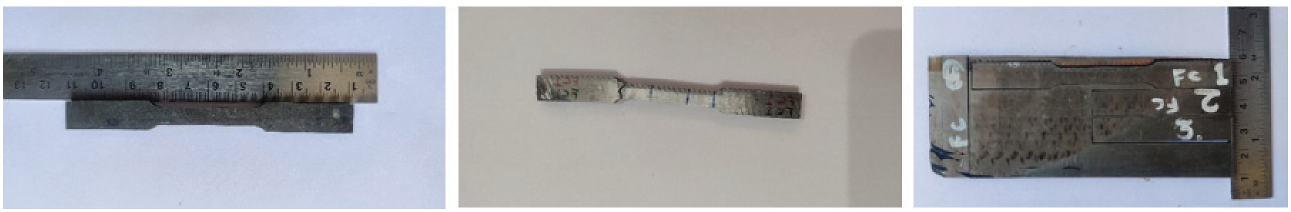

Before test Specimen After test Specimen Tensile Specimen

Figure 7. Sample for tensile specimen.

Table 3. Tensile properties of chrome moly steel as per standard grade and GMAW-based moly steel

Property	Ultimate tensile strength (MPa)	Yield strength (MPa)	Elongation%
GMAW-based moly steel	910.68	728.471	3.92
Chrome moly steel	890	712	19.9

impact values was detected, with the lower zone showing somewhat higher values than the upper zone.

The accelerated cooling rate in the lower region, caused by the cold plate and the environment, resulted in a slight increase in strength in this region. The ultimate tensile strength of chrome moly steel is 890 MPa, and its yield strength is 712 MPa. The GMAW-produced chrome molybdenum steel exhibited an ultimate tensile strength of 910 MPa and a yield strength of 728 MPa. These values are superior to those of commercially available chrome moly steel (Table 3).

The produced multi-layer formation demonstrates sufficient durability for prospective industrial applications.

CONCLUSION

The WAAM process using a GMAW source proved valuable for achieving a high deposition rate, favourable mechanical properties, and low equipment cost. In this study, the GMAW-based WAAM process was used to fabricate a multi-layered structure of chrome moly steel under optimal conditions. The study investigated how geometry, strength, and toughness of the multi-layered structure vary between the top and bottom zones.

The main findings are as follows: A suitable connection between adjacent layers was observed, with proper fusion and no oxidation. No defects were detected, and the macrostructure at various zones confirmed acceptable geometries. Equiaxed grains with small diameters predominated in the bottom zone's microstructure.

The ultimate tensile strength of chrome moly steel is 890 MPa, and its yield strength is 712 MPa. The GMAW-produced chrome molybdenum steel exhibited an ultimate tensile strength of 910 MPa and a yield strength of 728 MPa. These values are superior to those of commercially available chrome moly steel. The multi-layer formation produced by the WAAM process demonstrates sufficient durability for prospective industrial applications.

All tensile characteristics established by WAAM for the top and bottom zones fall within acceptable ranges. The results are comparable to those of commercially available chrome moly steel. The average impact strength of 5.3 J demonstrates adequate toughness. A slight variation in impact values was observed, with the bottom zone showing higher strength than the upper zone.

Overall, the results indicate that the structure fabricated using the GMAW-based WAAM technique meets industrial application requirements.

ACKNOWLEDGMENT

The authors are grateful to Parul University, Vadodara, and Pandit Deendayal Energy University, Gandhinagar, for providing the facilities and resources that greatly supported the experiments. Their steadfast support and invaluable assistance have been crucial to the success of this study. We appreciate their contributions and commend their dedication to advancing scientific research and academic excellence.

AUTHORSHIP CONTRIBUTIONS

Vaishali Prajapati: Writing – original draft and editing, conceptualization, investigation, formal analysis, Data curation, methodology, validation. **Vyomesh Buch**: Writing – review & editing, formal analysis, Supervision

Jay Vora: writing, review and editing, data curation, validation, supervision

DATA AVAILABILITY STATEMENT

The authors confirm that the data that supports the findings of this study are available within the article. Raw data that support the finding of this study are available from the corresponding author, upon reasonable request.

CONFLICT OF INTEREST

The author declared no potential conflicts of interest with respect to the research, authorship, and/or publication of this article.

ETHICS

There are no ethical issues with the publication of this manuscript.

STATEMENT ON THE USE OF ARTIFICIAL INTELLIGENCE

Artificial intelligence was not used in the preparation of the article.

NOMENCLATURE

AM	Additive manufacturing
GMAW	Gas metal arc welding
UTS	Ultimate tensile strength
SEM	Scanning electron microscopy

YS	Yield strength
WAAM	Wire arc additive manufacturing
TS	Tarvel speed
PVS	Passing vehicle search
DAS	Dendritic arm spacings

REFERENCES

[1] Rosli NA, Alkahari MR, Abdollah MFB, Maidin S, Ramli FR, Herawan SG. Review on effect of heat input for wire arc additive manufacturing process. J Mater Res Technol 2021;11:2127−2145. [CrossRef]

[2] Korkmaz ME, Waqar S, Garcia-Collado A, Gupta MK, Krolczyk GM. A technical overview of metallic parts in hybrid additive manufacturing industry. J Mater Res Technol 2022;18:384−395. [CrossRef]

[3] Huang SH, Liu P, Mokasdar A, Hou L. Additive manufacturing and its societal impact: A literature review. Int J Adv Manuf Technol 2013;67(5):1191−1203. [CrossRef]

[4] Senthil TS, Ramesh Babu S, Puviyarasan M, Dhinakaran V. Mechanical and microstructural characterization of functionally graded Inconel 825-SS316L fabricated using wire arc additive manufacturing. J Mater Res Technol 2021;15:661−669. [CrossRef]

[5] Nguyen HD, Pramanik A, Basak AK, Dong Y, Prakash C, Debnath S, et al. A critical review on additive manufacturing of Ti-6Al-4V alloy: Microstructure and mechanical properties. J Mater Res Technol 2022;18:4641−4661. [CrossRef]

[6] Hu Z, Qin X, Li Y, Yuan J, Wu Q. Multi-bead overlapping model with varying cross-section profile for robotic GMAW-based additive manufacturing. J Intell Manuf 2020;31:1133−1147. [CrossRef]

[7] Chaudhary B, Jain NK, Murugesan J, Patel V. Exploring temperature-controlled friction stir powder additive manufacturing process for multi-layer deposition of aluminum alloys. J Mater Res Technol 2022;20:260−268. [CrossRef]

[8] Shen B, Chen X, Wang J, Shi J, Tang X, Xu G. Multimodal-based weld reinforcement monitoring system for wire arc additive manufacturing. J Mater Res Technol 2022;20:561−571. [CrossRef]

[9] Dinovitzer M, Chen X, Laliberte J, Huang X, Frei H. Effect of wire and arc additive manufacturing (WAAM) process parameters on bead geometry and microstructure. Addit Manuf 2019;26:138−146. [CrossRef]

[10] Laleh M, Hughes AE, Xu W, Gibson I, Tan MY. Unexpected erosion-corrosion behaviour of 316L stainless steel produced by selective laser melting. Corros Sci 2019;155:67−74. [CrossRef]

[11] Moeinfar K, Khodabakhshi F, Kashani-Bozorg SF, Mohammadi M, Gerlich AP. A review on metallurgical aspects of laser additive manufacturing (LAM): Stainless steels, nickel superalloys, and titanium alloys. J Mater Res Technol 2022;16:1029−1068. [CrossRef]

[12] Khidhir GI, Baban SA. Efficiency of dissimilar friction welded 1045 medium carbon steel and 316L austenitic stainless steel joints. J Mater Res Technol 2019;8:1926−1932. [CrossRef]

[13] Isquierdo DV, Siqueira RHM, Carvalho SM, Lima MSF. Effect of the initial substrate temperature on heat transfer and related phenomena in austenitic stainless steel parts fabricated by additive manufacturing using direct energy deposition. J Mater Res Technol 2022;18:5267−5279. [CrossRef]

[14] Jin W, Zhang C, Jin S, Tian Y, Wellmann D, Liu W. Wire arc additive manufacturing of stainless steels: A review. Appl Sci 2020;10:1563. [CrossRef]

[15] Chen X, Li J, Cheng X, Wang H, Huang Z. Effect of heat treatment on microstructure, mechanical and corrosion properties of austenitic stainless steel 316L using arc additive manufacturing. Mater Sci Eng A 2018;715:307−314. [CrossRef]

[16] Queguineur A, Rückert G, Cortial F, Hascoët JY. Evaluation of wire arc additive manufacturing for large-sized components in naval applications. Weld World 2018;62:259−266. [CrossRef]

[17] Ahsan MRU, Tanvir ANM, Ross T, Elsawy A, Oh MS, Kim DB. Fabrication of bimetallic additively manufactured structure (BAMS) of low carbon steel and 316L austenitic stainless steel with wire + arc additive manufacturing. Rapid Prototyp J 2019;26:519−530. [CrossRef]

[18] Le VT, Mai DS. Microstructural and mechanical characteristics of 308L stainless steel manufactured by gas metal arc welding-based additive manufacturing. Mater Lett 2020;271:127791. [CrossRef]

[19] Fang Q, Xiang J, Wang J, Tan L, Su C, Wang K, et al. 800 MPa class HSLA steel block part fabricated by WAAM for building applications: Tensile properties at ambient and elevated (600°C) temperature. Adv Mater Sci Eng 2022;2022:3014060. [CrossRef]

[20] Long P, Wen D, Min J, Zheng Z, Li J, Liu Y. Microstructure evolution and mechanical properties of a wire-arc additive manufactured austenitic stainless steel: Effect of processing parameter. Materials (Basel) 2021;14:1681. [CrossRef]

[21] Singh S, Jinoop AN, Tarun Kumar GTA, Palani IA, Paul CP, Prashanth KG. Effect of interlayer delay on the microstructure and mechanical properties of wire arc additive manufactured wall structures. Materials (Basel) 2021;14:4187. [CrossRef]

[22] Savsani P, Savsani V. Passing vehicle search (PVS): A novel metaheuristic algorithm. Appl Math Model 2016;40:3951−3978. [CrossRef]

[23] Sunay N, Kaya M, Kaynak Y. Properties of parts fabricated by additive manufacturing. Sigma J Eng Nat Sci 2020;38:2027−2042.

[24] Gao C, Chen X, Su C, Chen X. Location dependence of microstructure and mechanical properties on wire arc additively manufactured nuclear grade steel. Vacuum 2019;168:108818. [CrossRef]

[25] ASTM International. Standard test methods for notched bar impact testing of metallic materials. ASTM E23-12c. West Conshohocken (PA): ASTM International; 2012.